JOURNAL OF THE HYDRAULICS DIVISION

THEORETICAL MODEL OF RIVER ICE JAMS

By Mehmet S. Uzuner,[1] A. M., ASCE and John F. Kennedy,[2] M. ASCE

BACKGROUND

Introductory Remarks.—Ice jams (embacles) confront river engineers with a variety of problems, including flooding caused by blockage of channels, damage to structures, interference with navigation, and obstruction of diversion intakes, to mention but a few. An Army Corps of Engineers survey (4) places the reported national annual average loss due to ice jams during the period 1963-1973 at $16,600,000, and estimates the actual annual loss to be in the vicinity of $80,000,000. Ice jamming is such a complex phenomenon, or to be more precise, ensemble of phenomena, that it is difficult even to frame a concise definition of an ice jam. Detailed descriptions of specific ice jams have been reported by the Corps of Engineers (7), Frankenstein (5), and Frankenstein and Assur (6). The writers (12) previously proposed a definition which, with slight modification, reads as follows. An ice jam is an accumulation of ice on a stream which produces extensive blockage of the channel; the accumulation generally is initiated by an obstruction, which may consist of arrested ice, a change in channel alinement or cross section, or natural or man-made obstacles in the stream. Fig. 1 shows an ice jam initiated by bridge piers. The writers (12) have presented a compilation of circumstances that can produce embacles.

The analytical study reported herein had as its principal goal the development of a mathematical model for the prediction and presentation of data on the velocity of upstream propagation of jams, the streamwise distributions of flow depth and jam thickness, the normal and shear stresses in the jammed ice, and the time required for evolution of jams to equilibrium (quasi-steady) conditions. the differential equations underlying the analysis developed in the next section are the static force equilibrium formulation for the ice cover, the unsteady nonuniform momentum relation for the flow beneath and approaching the jam, and the unsteady continuity equations for the liquid and frozen water.

Note.—Discussion open until February 1, 1977. To extend the closing date one month, a written request must be filed with the Editor of Technical Publications, ASCE. This paper is part of the copyrighted Journal of the Hydraulics Division, Proceedings of the American Society of Civil Engineers, Vol. 102, No. HY9, September, 1976. Manuscript was submitted for review for possible publication on February 27, 1975.

[1]Consulting Hydr. Engr., ARCTEC, Inc., Columbia, Md., formerly, Research Assoc., Inst. of Hydr. Research, Univ. of Iowa, Iowa City, Iowa.

[2]Dir., Inst. of Hydr. Research, Univ. of Iowa, Iowa City, Iowa.

Relations between cover thickness and the compressive and shear strengths of floating fragmented ice covers are then introduced into the force and momentum equations to obtain a set of simultaneous equations which was solved numerically. A fairly complete set of results for a specific example is presented graphically.

Genesis and Evolution of Ice Jams.—In order to gain a better appreciation of the several constituent phenomena that result in ice jamming and further

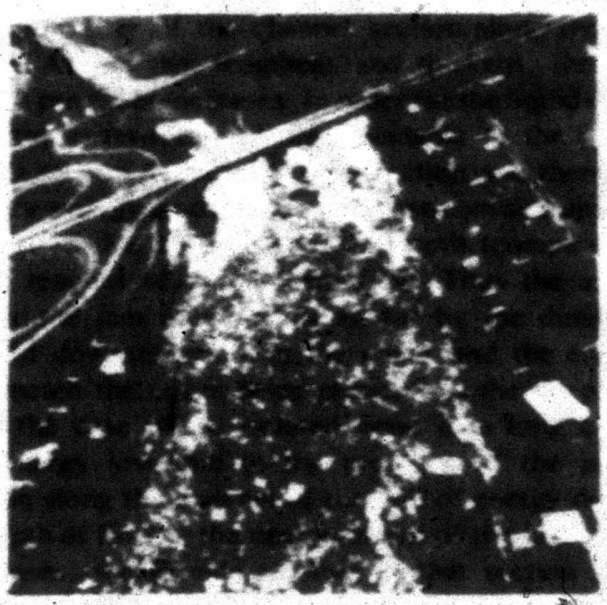

FIG. 1.—Aerial Photograph of March 1972, Ice Jam Initiated by I-80 Bridge, on Rock River Just Upstream from Its Confluence with Mississippi River, near Rock Island, Ill.

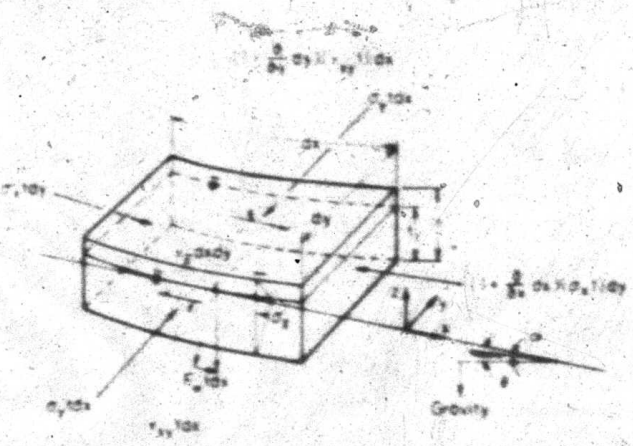

FIG. 2.—Control Volume Showing Forces Exerted on and within Ice Jam

insight into the mechanics of jams, a rather complete description of the genesis and evolution of a typical jam will be presented herein. The analysis will be limited to a uniform rectangular channel of very great depth (the large depth being included to permit the depth of flow plus the ice thickness to increase indefinitely without the added complication of overbank flow). As noted previously, a jam is initiated when the downstream passage of floating ice being

transported by a stream is impeded. An obstacle to passage of subsequent floes arriving at the section is produced, and the stage is set for development of a jam.

The stability of arriving ice blocks against submergence, which has been described and analyzed in detail by the writers (12), Ashton (1), and the first writer (11), depends on the flow conditions and floe geometry. The blocks swept under the cover may come to rest near the upstream end of the cover to form a "hanging dam," or be transported farther downstream, either coming to rest at some location or possibly (but not usually) being swept under the arrested ice, past the channel obstruction, and continuing downstream.

The ice cover produces an additional localized energy loss by lengthening the wetted perimeter of the channel section along the reach occupied by the arrested ice. As the jam lengthens and thickens, the magnitude of the flow obstruction it produces increases. In order for the liquid discharge to pass beneath the cover, the cross-sectional area available to the flow is increased by the ice "floating up" to deepen the flow section and thereby reduce the velocity. Moreover, the energy gradients just downstream and upstream from the evolving jam are reduced due to the increased depth (compared to the normal depth) along these reaches of nonuniform flow. Thus the added resistance to flow produced by the jam is compensated for by the diminished energy gradients upstream and downstream from the cover and the energy dissipation rate of the flow beneath the cover being reduced by the deepening of the flow. Note that, as in the case of an isolated bend in a long channel, there is no net additional energy loss due to the presence of the jam, but, rather, only a redistribution along the channel of the rate of energy dissipation.

As the depth of flow at the upstream end of the jam increases and the velocity there decreases, the Froude number at that section decreases and, thus, so also do the ability of the flow to submerge ice blocks reaching the jam and the momentum of the arriving floes. A depth is eventually reached above which the arriving floes are no longer submerged, but come to rest at the upstream edge of the jam, causing it to lengthen in the upstream direction. The development and upstream propagation of the backwater profile results in storage of a significant volume of water and consequently reduces liquid discharge just upstream from and beneath the jam.

The principal external forces applied to the ice field are the streamwise component of the weight of the ice cover and the pore water it contains, the shear force applied by the flowing water to the bottom of the cover, and the impact of the arriving floes. These forces are balanced by the longitudinal gradient of the internal effective normal force acting on planes oriented perpendicular to the flow direction and the shear forces exerted on the ice by the banks. It is reasonable to expect that both the shear and normal strengths of the cover will increase as it thickens. Now as the length of the jam is increased by the capture of newly arrived floes, the total streamwise external force applied to the jam upstream from any section will cause the jam to thicken by failure or "collapse" of the ice accumulation (and generally not by fracture of the individual floes) until its shear and compressive strengths become great enough to support the applied forces. At large distances downstream from the upstream end of the jam, the cover will become sufficiently thick so that just the bank shear will be equal to the applied external forces, both per unit length of channel.

and no streamwise gradient in the compressive force, nor therefore in the jam thickness, will be required. Where this balance attains the embacle is said to have reached its equilibrium thickness. Note that the jam still may be lengthening, due to arrival of more ice, and thickening to equilibrium along its nonuniform reach. Over the downstream reach where the jam has attained equilibrium the slope of the energy grade line must be close or equal to that of the channel. Once the jam has attained its equilibrium thickness at some point, its subsequent development is quasi-steady, i.e., when viewed in a coordinate system moving upstream with velocity equal to that of the leading edge, both the jam profile and the flow field appear steady.

The evolution of an embacle was examined previously without consideration of limitations on its development. Generally, ice will continue to accumulate in a jam until the supply from upstream is exhausted. Therefore if the volume of ice moving into the jammed reach and the distribution of ice-cover thickness along its length are known, the upstream extent of the jam from the obstacle and the increase in river stage it will produce can be determined. The analytical framework for this calculation is developed later.

Natural stream channels generally do not have vertical sides and effectively unbounded depth, but rather are characterized by gently sloping banks. Consequently, as a jam evolves and the water depth increases, the flow will occupy a progressively wider channel. This gives the flow system an added degree-of-freedom and significantly complicates the analysis of ice jams. In a severely jammed river, significant portions of the liquid and ice discharges may occur outside of the main channel, in the overbank areas. In a complete analysis of a specific jam, the cross sections of the particular river channel and valley must be taken into consideration, and the transport and storage of liquid water and ice in the overbank regions accounted for. A further complication then arises in the formulation of the force balance in the jam, since the lateral constraint condition is no longer well defined, and the simplifications of a one-dimensional analysis cannot be employed. The ensuing analysis is limited to the one-dimensional situation.

Formulation of Theoretical Model

Force Equilibrium in Floating Fragmented Ice Cover.—Consider an element of rectangular plan form taken from an ice cover floating on a flowing stream, as depicted in Fig. 2, in which the coordinate axes and the notation adopted for several of the quantities arising in the analysis are defined. The x-axis is parallel to, and the lateral faces of the control volume are normal to, the phreatic surface in the cover. The normal stresses, σ_x and σ_z, and the shear stress, τ_{xz}, in the ice are effective values averaged over the ice cover thickness. The internal surface forces actually are transmitted by particle-to-particle contact, but the stresses are calculated on the basis of the transmitted force divided by the entire surface area (and not just the interparticle contact area). It is assumed that on every point the z component of the weight of the cover is supported by buoyancy; in other words, there are no bending stresses in the cover. The force balance in the y direction is of no particular interest here except as it affects the normal stress on x-z planes, σ_z, which in turn plays a role in determining τ_{xz}, which will be considered later.

The x component of the weight of the ice and the pore water it contains, per unit area in the x-y plane, is

$$F_w = \left[t(1-p)\frac{\rho'}{\rho} + t_2 p \right] \rho g \sin(\theta + \alpha) \quad \ldots\ldots\ldots\ldots\ldots\ldots\ldots (1)$$

in which $(\theta + \alpha)$ = the slope of the phreatic line; ρ and ρ' = the densities of liquid and frozen water, respectively; g = the gravitational constant; and p = the porosity. Equating the z components of the weight of the ice above the phreatic surface to the buoyant weight of the submerged ice yields

$$t(1-p)\rho' g \cos(\theta + \alpha) = t_2 (1-p)\rho g \cos(\theta + \alpha) \quad \ldots\ldots\ldots\ldots\ldots\ldots (2)$$

Substituting t_2, obtained from Eq. 2, into Eq. 1 gives

$$F_w = \rho' g t \sin(\theta + \alpha) \quad \ldots\ldots\ldots\ldots\ldots\ldots\ldots\ldots\ldots\ldots (3)$$

Note from Eq. 2 that the slope of the water surface and that of the bottom of the ice cover differ only by $(\rho'/\rho)(\partial t/\partial x)$.

The balance of the forces depicted in Fig. 2 and given by Eq. 3 acting on the control volume in the x direction is expressed by

$$\frac{\partial}{\partial x}(t\sigma_x) - \frac{\partial}{\partial y}(t\tau_{xy}) - \tau_2 \cos\left(\frac{\rho'}{\rho}\frac{\partial t}{\partial x}\right) - \rho' g t \sin(\theta + \alpha) = 0 \quad \ldots\ldots (4)$$

for a laterally uniform jam [i.e., for the case $(\partial/\partial y)(t, \tau_2) = 0$]. Note that the x components of the hydrostatic pressure forces acting on the surface of the control volume are themselves in balance. Before Eq. 4 can be integrated to obtain t as a function of x and time, it is necessary to express σ_x, τ_2, and τ_{xy} as functions of t.

Effective Stresses in Floating Fragmented Covers.—Consider again the element depicted in Fig. 2 taken from a floating fragmented ice cover. As the external loads applied through τ_2 and F_w are increased, a point will be reached beyond which the strength of the cover, reflected in the limiting values of σ_x and τ_{xy}, is inadequate to support the external loading. The cover then will fail, and rearrangement of the fragments and accompanying thickening of the jam will occur until the internal surface forces are adequate to support the externally applied loads. It should be borne in mind that the cover will not thicken by this process until its strength is exceeded, i.e., it will not be dependent on the loading until the onset of failure. The thickening of the cover will be resisted by gravitational forces reflected in the normal stress acting on x-y planes, σ_z, and by the cohesive strength of the interparticle bonds, which also are dependent on σ_z (as well as on several other quantities). Accordingly, it is of interest to examine σ_z. For $z > 0$

$$(\sigma_z)_{z>0} = \rho' g \left[\left(1 - \frac{\rho'}{\rho}\right) t - z \right] (1-p)\cos(\theta + \alpha) \quad \ldots\ldots\ldots\ldots\ldots\ldots (5)$$

while for $z < 0$

$$(\sigma_z)_{z<0} = g(\rho - \rho')(1-p)\left(\frac{\rho'}{\rho}t + z\right)\cos(\theta + \alpha) \quad \ldots\ldots\ldots\ldots\ldots\ldots (6)$$

The average value of σ_x over the whole thickness, σ_{x_a}, is

$$\sigma_{x_a} = \frac{t}{2}\left(\rho - \frac{\rho^2}{\rho'}\right)(1-p)\rho' g\cos(\theta+\alpha) = \gamma_e t \quad (7)$$

in which $\gamma_e = (1/2)[1-\rho'/\rho)(1-p)\rho' g\cos(\theta+\alpha)$.

It will be assumed that when the ice field is undergoing failure by displacement of the fragments relative to each other

$$\sigma_y = k_a\sigma_{x_a}, \quad \sigma_y = k_a\gamma_e t \quad (8)$$

and that the shear strength can be expressed in the form of Coulomb's law for granular materials

$$(\tau_{xy})_M = C_\phi\sigma_y + C_c, \quad (\tau_{xy})_M = C_\phi\gamma_e t + C \quad (9)$$

in which k_a = a stress ratio-that is analgous to Rankine's passive stress coefficient; C_ϕ = a shear stress coefficient; C = the cohesive intercept described by Lambe and Whitman (8); and $(\tau_{xy})_M$ = the failure value of τ_{xy}. Eq. 9 it has also been assumed that the lateral normal stress, σ_y, which gives rise to the friction component of the strength, is proportional to σ_x. Further justification for the adoption of Eqs. 8 and 9 is given by the first writer (11) and Merino (10). Suffice it herein to note that k_a and C_ϕ, and likely also C_c, are strongly strain-rate dependent for ice. The first writer's (11) experimental results indicate that k_a varies inversely with the mean linear compressive strain rate from about 12 for strain rates greater than roughly 2×10^{-4} sec^{-1} to 100 at strain rates in the neighborhood of 10^{-5} sec^{-1}. Merino's (10) shear-strength experiments yielded a consistent value of C_c of about 2 psf (9.76 kg/m^2). The coefficient, C_ϕ, on the other hand, was found by Merino (10) to range from about 2-100 as the shear-strain rate (based on an average ice-fragment dimension) was varied from about 0.015 sec^{-1}-0.4 sec^{-1}, and tends toward zero as the reciprocal of the strain rate as the deformation rate was increased. However, these three coefficients will be treated as constants in the present analysis, because the understanding of their behavior is inadequate to justify greater refinement.

In the case of a straight prismatic channel, τ_2 is uniformly distributed under the ice cover. The internal stress, τ_{xy}, however, varies linearly across the stream, in the y direction. This can be seen from Eq. 4 when it is remembered that t, σ_x, and τ_2 are independent of y. Therefore, $\partial\tau_{xy}/\partial y$ is constant at a fixed location along the stream. $\tau_{xy} = 0$ at $y = 0$ (the midplane of the channel) because of symmetry. Therefore τ_{xy} is

$$\tau_{xy} = -\frac{2y}{W}(\tau_{xy})_M \quad (10)$$

in which W = the width of the channel. Eq. 10 implies that shear failure of the ice accumulation occurs at the banks.

Nondimensional Force-Equilibrium Relation.—Substituting Eqs. 7, 8, 9, and 10 into Eq. 4, carrying out the indicated differentiation, and normalizing by setting

$$x_n = \frac{x}{h_e} \quad \text{and} \quad t_n = \frac{t}{h_e} \quad (11)$$

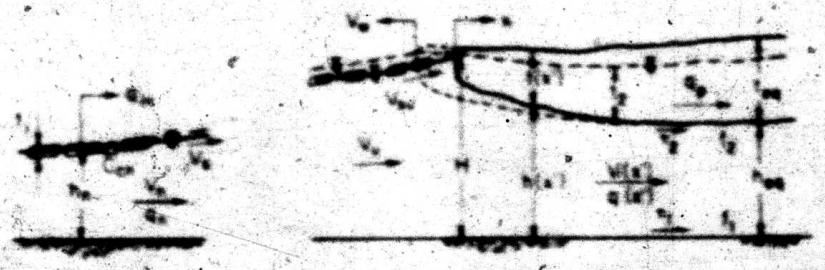

FIG. 3.—Longitudinal Section through Quasi-Steady Ice Jam and Approaching Flow

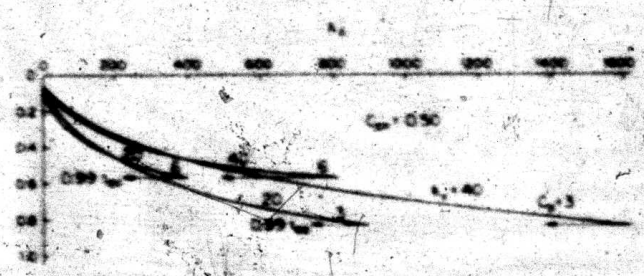

FIG. 4.—Normalized Jam-Thickness Profiles for Different Values of k_s and C_o

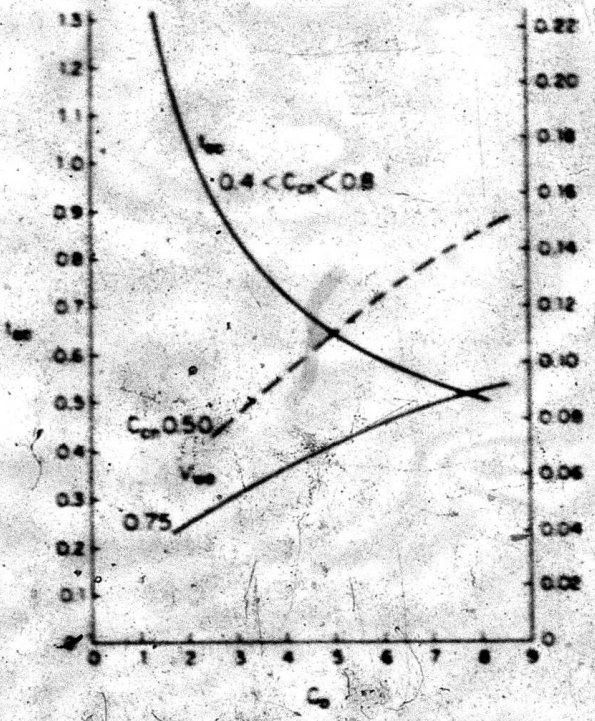

FIG. 5.—Relationships Between t_{wo}, V_{wo}, C_o, and C_{co}

in which h_n = the normal depth for the flow, given by

$$h_n = \left(\frac{f_i\, q_n^2}{8\, g\, S_n}\right)^{1/3} \qquad (12)$$

in which $q_n = V_n\, h_n$ = the unit discharge far upstream (see Fig. 3); f_i =

the Darcy-Weisbach friction factor related to the streambed, and $S_o = \sin\theta$ = the channel slope, leads to

$$t_* \frac{\partial t^*}{\partial x^*} = a + b t^* + c t^{*2} \quad \ldots\ldots (13)$$

in which $a = \frac{\tau_2}{2 k_s \gamma_s h_*}$ $\ldots\ldots (14)$

$$b = \frac{\rho' g S_o - 2 \frac{C_0}{W}}{2 k_s \gamma_s} \quad \ldots\ldots (15)$$

and $c = -\frac{C_0 h_*}{k_s W}$ $\ldots\ldots (16)$

Note that in Eq. 14 τ_2 is a function of depth of flow beneath the cover, h (see Fig. 3). Its determination requires analysis of the flow beneath the jam, as follows.

Gradually Varied Unsteady Flow Under Floating Ice Cover.—In this section the unsteady momentum equation for nonuniform flow under an ice cover is derived in order to determine the streamwise distributions of flow depth, mean velocity, and shear stress under the arrested ice. From Fig. 3 and Eq. 2 it is seen that the continuity equation for the liquid flow through and beneath the ice cover is

$$\frac{\partial q}{\partial w}\frac{\partial h}{\partial T} + \rho \frac{\rho'}{\rho}\frac{\partial t}{\partial T} + \frac{\partial q_p}{\partial x} = 0 \quad \ldots\ldots (17)$$

in which q and q_p = the water discharges per unit width under the cover and through the jammed ice; $h(x, T)$ = the flow depth beneath the cover; and T = time. The momentum balance for the control volume of unit width bounded by the streambed and the bottom of the cover is expressed by

$$\frac{\partial}{\partial x}\left[(2 t \rho' g + \rho g h)\frac{h}{2}\cos\theta\right] + (\tau_1 + \tau_2) - t \rho' g \frac{\partial h}{\partial x}\cos\theta - \gamma h S_o + \frac{\partial}{\partial T}(\rho V_s h) + \frac{\partial}{\partial x}(\rho V^2 h) + \rho V\left(\frac{\partial q_p}{\partial x} + \rho \frac{\rho'}{\rho}\frac{\partial t}{\partial T}\right) = 0 \quad \ldots\ldots (18)$$

Note that in Eq. 18 the x-axis has been taken as parallel to the plane streambed, which implies $\alpha << \theta$; this restriction will be retained hereinafter, as will the approximation $\cos\theta \approx 1$. The first term on the left-hand side of Eq. 18 arises from the hydrostatic pressure distributions acting on the control volume in the streamwise direction, while the third term on the left is the x component of the force exerted by the weight of the ice and its pore water. The last term on the left-hand side of Eq. 18 represents the momentum flux through the bottom of the ice cover.

After the jam reaches equilibrium thickness at its downstream end, its leading edge will propagate upstream with constant velocity. This can be seen from

consideration of the continuity of ice movement if the arriving floes are envisioned as merely increasing the length of the equilibrium reach. It is then apparent that the upstream end of the jam will move with constant velocity, provided the ice discharge reaching the jam also is constant, and the volume of ice contained in the jam upstream from the point where the equilibrium thickness has just been reached remains constant. The jam and flow then appear steady in a coordinate system moving upstream with speed equal to that of the jam front, V_u. In this case, the time derivatives in the continuity and momentum relations, Eqs. 17 and 18, can be replaced by

$$\frac{\partial}{\partial T} = V_u \frac{d}{dx'} \quad \ldots \quad (19)$$

in which $x' = x + V_u T$ = the new streamwise coordinate. Utilization of Eq. 19 in Eqs. 17 and 18, elimination between the resulting two equations of the last two terms in each, and normalization by $\rho g h$ of the expression so obtained results in

$$\frac{\rho'}{\rho}\frac{dt}{dx'} + \left(1 - \frac{V'^2}{gh}\right)\frac{dh}{dx'} + S_f - S_0 = 0 \quad \ldots \quad (20)$$

in which $V' = V + V_u = q/h + V_u$; and $S_f = (\tau_1 + \tau_2)/\rho g h$. Eq. 20 is the continuity-momemtum relation for the flow beneath the ice cover in a coordinate system moving upstream with velocity V_u. For $t = 0$, Eq. 20 reduces to the classical equation of gradually varied flow.

The simultaneous solution of the equations expressing the force balance in the jam, Eq. 4, and the continuity-momentum equation for the flow, Eq. 20, yields h and t as a function of x' for a quasi-steady jam. Before this can be accomplished, however, it is necessary to obtain an expression for V_u and formulate the boundary conditions.

Determination of V_u, Reduced Water Discharge Beneath Jam, Equilibrium Values of h and t, and Upstream Boundary Condition on t.—As the jam front moves upstream a significant quantity of water is stored in the backwater profile, which propagates upstream as a monotonic wave, and under the lengthening jam. As a result, the actual liquid discharge (measured in fixed coordinates) under the ice and downstream from the jam is reduced. This effect has been observed in natural ice jams by Bojurnas (3) and Larsen (9). The reduced discharge must be used in calculating the shear stress acting on the jam, τ_2, and the energy gradient, S_f.

Determination of V_u.—For a quasi-steady jam, conservation of the volume of ice moved downstream by the flow is expressed by

$$q_i' = q_{in} + C_{cn} t_i V_u; \quad q_i' = C_{ci} t_i (V_u + V_u) \quad \ldots \quad (21)$$

in which, as shown in Fig. 3, q_{in} and C_{cn} = the ice discharge per unit width and surface concentration far upstream, where the flow is uniform at its normal depth; t_i = the floe thickness; and q_i' = the ice discharge in moving coordinates across any section, including that at the leading edge of the jam. Another expression for q_i' may be obtained by noting that after equilibrium thickness is reached, ice accumulates in the jam at the following rate

$$q_i = V_* t_{eq} (1 - p) \quad (22)$$

in which t_{eq} = the equilibrium thickness of the jam. Eqs. 21 and 22 yield

$$V_* = \frac{q_{in}}{t_{eq}(1 - p) - C_{in} t_i} \quad (23)$$

Determination of q.—If the discharge through the ice is neglected, the unit liquid discharge in the moving coordinate system, q', is

$$q' = (V_* + V_*) h_* = V' h \quad (24)$$

The discharge in fixed coordinates obtained from Eq. 24 is

$$q = (V' - V_*) h = q_* + V_* (h_* - h) \quad (25)$$

Determination of t_{eq} and h_{eq}.—Along the equilibrium reach, in which $\partial t_e / \partial x_e = 0$, the force equilibrium relation, Eq. 13, reduces to a quadratic equation for t_e, for which the physically meaningful solution is

$$t_{en} = \frac{-b - \sqrt{b^2 + 4ac}}{2c} \quad (26)$$

in which a, b, and c are defined by Eqs. 14, 15, and 16, respectively; and $t_{en} = t_{eq} / h_*$. The shear stress, τ_2, appearing in Eq. 14 can be obtained from the Darcy-Weisbach relation as

$$\tau_2 = \rho \frac{f_2 q^2}{8 h^2} \quad (27)$$

in which f_2 = the friction factor related to the bottom of the ice cover. Over the equilibrium reach, in which $\partial t / \partial x$ and $\partial h / \partial x = 0$, the slope of the energy grade line must be close or equal to that of the channel. The continuity-momentum relation, Eq. 20, then reduces to

$$S_f = S_o = \frac{q^2}{8 g h_*^3 h_{en}^3} (f_1 + f_2) \quad (28)$$

in which $h_{en} = h_{eq} / h_*$ = the normalized flow depth in the equilibrium reach.

The unknown quantities in Eqs. 23, 25, 26, and 28 are V_*, q, t_{en}, and h_{en}. Substitution of Eq. 27 into Eq. 26 gives an expression for t_{en} as a function of h. Using this expression for t_{en} in Eq. 23 gives V_* as a function of h which, when substituted into Eq. 25, gives $q(h)$. Finally, introducing $q(h)$ into Eq. 28 yields

$$h_{en} = \frac{1}{h_*} \left(\frac{f_1 + f_2}{8 g S_o} \right)^{1/3} \left[q_* - \frac{q_i (1 - h_{en})}{m} \right]^{2/3} \quad (29)$$

in which $m = \dfrac{-b - \sqrt{b^2 - 2ce h_{en}}}{2c} - C_{en} \dfrac{t_i}{h_*}$ (30)

and $e = \dfrac{f_2}{f_1 + f_2} \dfrac{\rho g}{\gamma_e} \dfrac{S_o}{k_s}$ (31)

Eq. 29 was solved numerically for h_{∞} using Wegstein's iteration technique (11). The determination of q, t_{∞}, and V_{∞} are then straightforward calculations from Eqs. 25, 26, and 23, respectively.

Upstream Boundary Condition on t.—The ice blocks reaching the upstream end of an ice jam are moving downstream with the surface velocity of the stream in front of the ice cover, V_{∞}. The leading edge thickness of the jam must be sufficient to withstand the momentum of the arriving floes. The equation expressing this dynamic condition is

$$\rho' q_i (V_{\infty} + V_{\infty}) = (\sigma_i t) \quad \text{at} \quad x' = 0 \qquad (32)$$

in which, from Eq. 25

$$V_{\infty} = \frac{q_{\infty} + V_{\infty}(h_{\infty} - H)}{H} \qquad (33)$$

in which $H = h(0) + (\rho'/\rho)\, t(0)$ = the flow depth immediately upstream from the jam. Note that at the upstream end of the cover, $x' = 0$, the flow depth is treated as changing abruptly from H–$h(0)$.

Presentation and Analysis of Results for Quasi-Steady Conditions

Calculational Procedure.—The numerical solution of the governing equations was handled in the following way. Eqs. 13 and 20 expressed in nondimensional terms in moving coordinates are, respectively

$$\frac{dt_o}{dx'_o} = \frac{1}{t_o}(a + b\, t_o + c\, t_o^2) \qquad (34)$$

and

$$\frac{dh_o}{dx'_o} = \frac{h_o^3 S_{\infty} - \dfrac{F_{\infty}^2 (f_1 + f_2)(1 + V_{\infty o} - V_{\infty o} h_o)^2}{8} - \dfrac{\rho'}{\rho}\left(\dfrac{dt_o}{dx'_o}\right) h_o^3}{h_o^3 - (1 + V_{\infty o}^2) F_{\infty}^2} \qquad (35)$$

in which $F_{\infty} = V_{\infty}/\sqrt{g h_{\infty}}$ = the Froude number of the approach flow; $h_o = h/h_{\infty}$; $V_{\infty o} = V_{\infty} h_{\infty}/q_{\infty}$; and $x'_o = x'/h_{\infty}$. The quantity, dt_o/dx'_o, was eliminated from Eq. 35 by substitution of Eq. 34, and the independent variable, x'_o, then was removed from the resulting relation and Eq. 34 by division to obtain a first-order nonlinear differential equation relating h_o and t_o. This relation was integrated numerically using the modified Adams-Bashfort method (2). The numerical integration was initiated at the upstream end of the equilibrium reach: $x'_o = x'_{\infty}$; $t_o = t_{\infty}$, in which dt_o/dx'_o and $dh_o/dx'_o = 0$. The difficulties that arise from the resulting indeterminacy of dt_o/dh_o (the ratio of the quantities given by Eqs. 34 and 35) were circumvented by means of l'Hospital's rule. The integration proceeded upstream to the point where $t_o = t(0)/h_{\infty}$ obtained from Eqs. 32 and 33. After the numerical relation between t_o and h_o was obtained, it was a straightforward calculation to determine x'_o as a function of t_o from Eq. 34. The incremental length, $\Delta x'_o$, for the first numerical step was calculated

using $t_{ss} = 0.99\, t_{sm}$ and the corresponding h_{ss} in order to avoid the difficulties arising from dt_{ss}/dx_{ss} being zero at $t_{ss} = t_{sm}$. The depth, h_{ss}, could then be calculated as a function of x_{ss} from the known relation between h_{ss} and t_{ss}. A computer program for accomplishing these calculations has been developed by the first writer and is described by him in considerable detail.

Illustrative Results.—An illustrative set of results is presented in Figs. 4–10 for several values of k_x, C_{ss}, C_{sm}, and the following channel, flow, and ice properties: $W = 1{,}000$ ft (304.8 m); $S_o = 0.0004$; $q_w = 39.5$ sq ft/sec (3.67 m^2/s); $h_w = 6.72$ ft (2.05 m); $F_w = 0.4$; $f_1 = 0.02$; $f_2 = 0.1$; $C_i = 2$ psf (9.76 kg/m²); $t_{ss} = t_i/h_w = 0.05$; and $p = 0.4$. Fig. 4 shows normalized ice thickness profiles extending downstream to the point where $t_{ss} = 0.99\, t_{sm}$. For the previous conditions and those in Fig. 4 it was found that the t_{ss} profiles are practically independent of C_{ss} over the range $0.4 < C_{ss} < 0.8$, the differences appearing

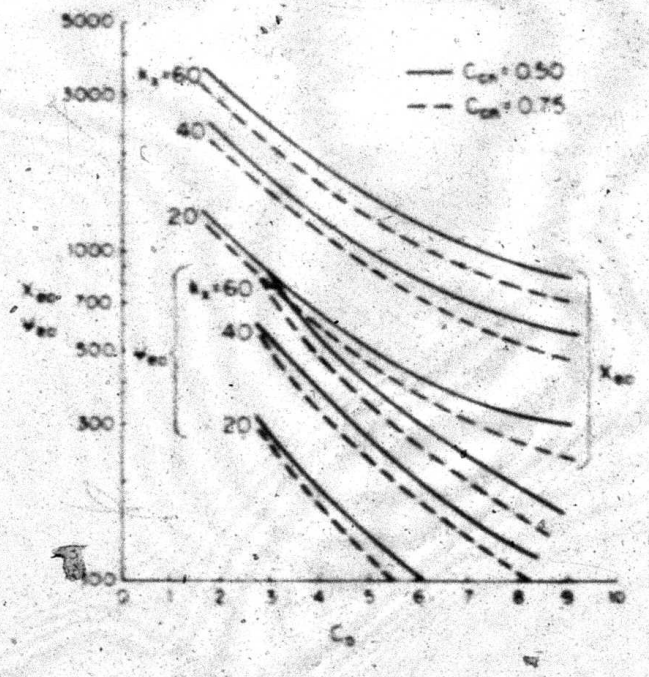

FIG. 6.—Normalized Length of and Volume of Ice Contained in Nonuniform Reach of Quasi-Steady Jam, as Functions of C_o, k_x, and C_s

principally in $t_{ss}(0)$ and x_{sm}. Note in Fig. 4 that t_{sm} is independent of k_x; it is also practically independent of C_{ss}, as can be seen in Fig. 5, in which the $t_{sm} - C_o$ relation given by Eq. 26 is presented. The nondependence of t_{sm} on k_x is, of course, a consequence of the externally applied forces being balanced by just the bank shear in the equilibrium reach. The slight dependence of t_{sm} on C_{ss} arises from the decrease of q (in fixed coordinates), and thus also of τ_{ss}, with increasing upstream ice concentration, which gives rise to larger V_{ss}. Fig. 5 also shows V_{sm} calculated from Eq. 23. As C_{ss} increases with the flow conditions held constant, the rate at which ice reaches the upstream end of the cover and accumulates in the jam will also increase; thus, the dependence of V_{sm} on C_{ss}. The normalized length of the nonuniform reach, $x_{sm} = x_{sm}/h_w$, in which internal normal and shear forces both act to balance the applied forces, is, unlike t_{sm}, strongly dependent on k_x, as can be seen in Figs. 4 and 6. Also

included in Fig. 6 is $\forall_{ss}$, the volume of ice, normalized by h_o^2, per unit width of channel contained in the jam upstream from x_{ss} in which $t_x = 0.99\ t_{ss}$). This volume was obtained by numerical integration of the thickness profile, multiplied by $(1 - p)$ to account for the porosity of the jam, using the trapezoidal rule. The quantity, $\forall_{ss}$, depends, of course, on the same quantities that determine the jam profile.

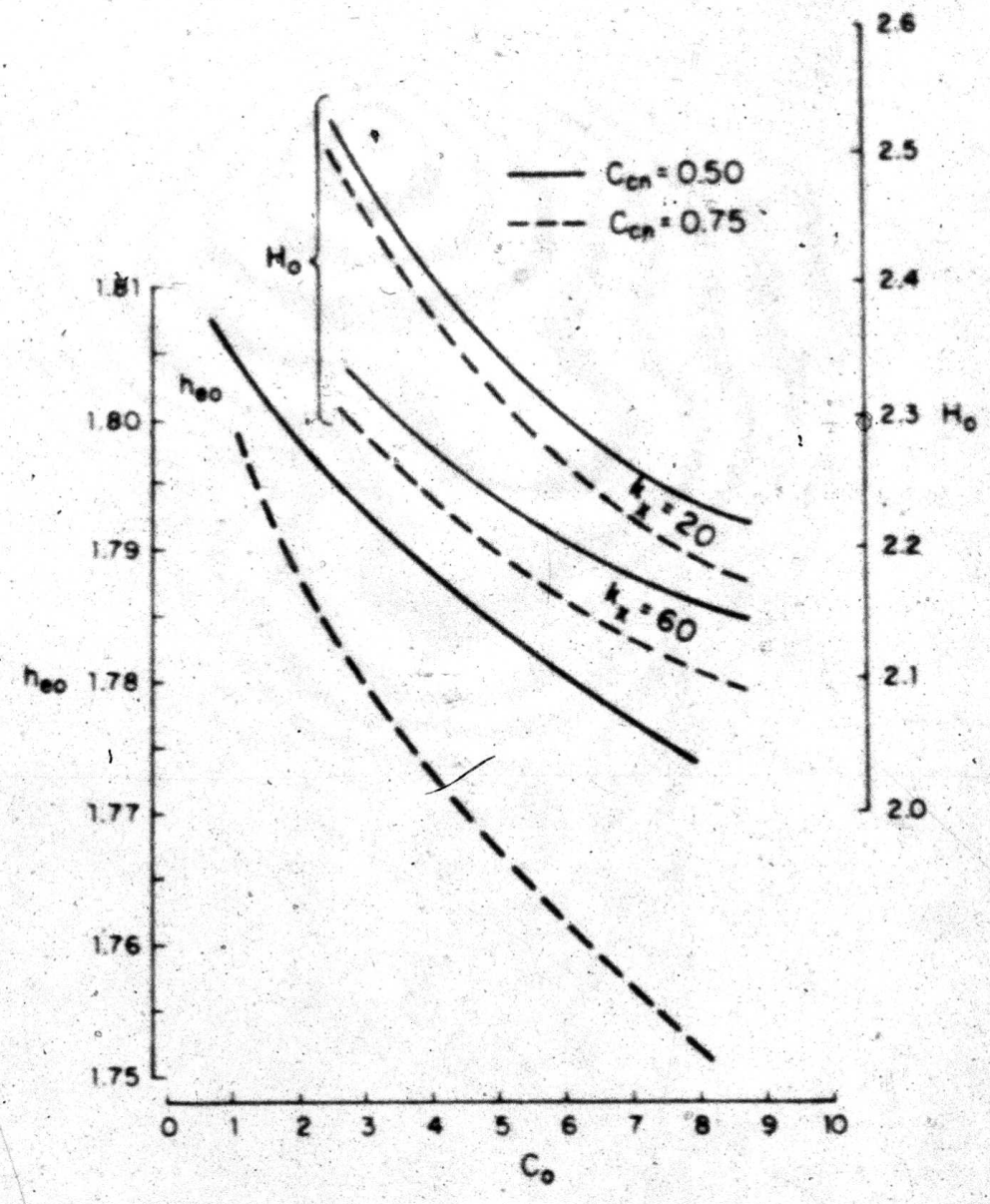

FIG. 7.—Variation of h_{ss} and H_o with C_o for Two Values of k_x and C_{cn} (Note h_{ss} is Practically Independent of k_x)

The equilibrium flow depth, h_{ss}, shown in Fig. 7, varies with both C_{cn} and C_o. The first of these dependencies arises from the fact that as V_{ss} increases with increasing C_{cn}, the discharge (measured in fixed coordinates) under the ice decreases, and thus so also does h_{ss}. The second results from increases in C_o reducing t_{ss}. However, Eq. 23 demonstrates that V_s increases with reduced

t_{eo}, leading to further reduction in the discharge beneath the ice, and therefore also in h_{eo}. Fig. 7 also gives $H_o = H/h_o$ as a function of k_s, C_{cw}, and C_o. From the manner in which H_o was calculated, by integration of the ice cover force balance and the flow momentum relations in the upstream direction from

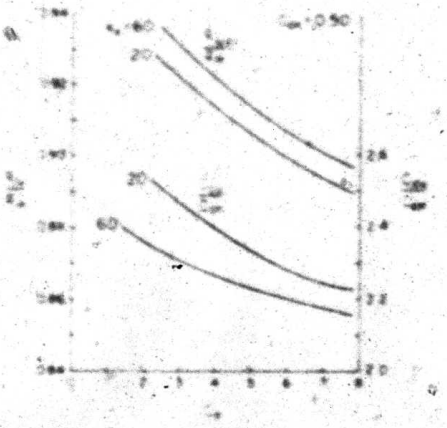

FIG. 8.—Normalized Ice Discharge and Ice Concentration at Upstream End of Ice Jam, as Functions of C_o and k_s for $C_{cw} = 0.50$

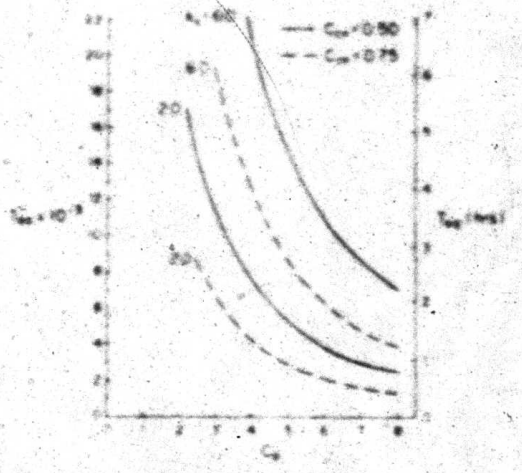

FIG. 9.—Time Required for Jam to Reach Quasi-Steady Conditions, as Function of C_o, k_s, and C_{cw}

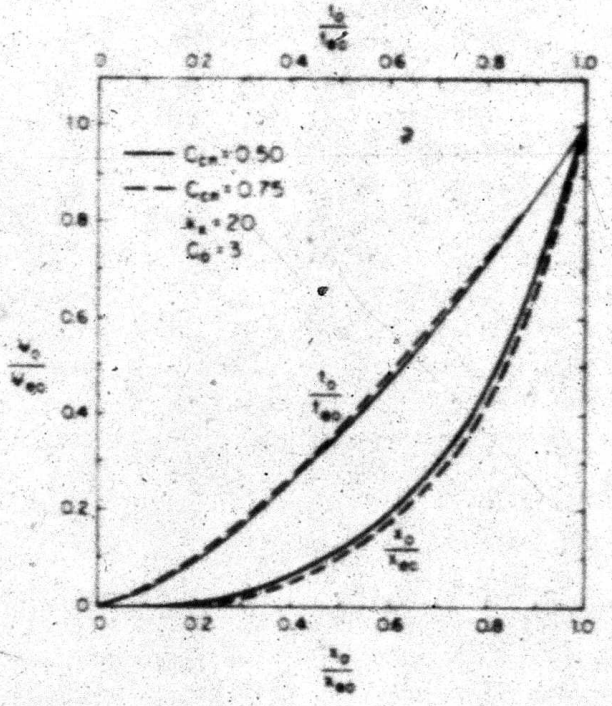

FIG. 10.—Distributions of Normalized Ice Volume and Normalized Jam Thickness Along Nonuniform Reach of Quasi-Steady Embacle

$x_o = x_{eo}$, in which $h_o = h_{eo}$, to the point where t_o satisfies the boundary condition expressed by Eqs. 32 and 33, and from consideration of the energy

equation of the flow, it is clear that H_o depends on h_{oo}, the flow depth profile over the nonuniform reach (which is a function of k_s, C_{co}, and the parameters describing the flow and channel), and the quantities that determine the upstream thickness, $t_o(0)$. It is apparent that H_o, like h_{oo}, will be heavily dependent on f_2/f_1.

Along the backwater reach leading to the jam the ice concentration, C_c, and ice discharge, q_i, measured in fixed coordinates, vary between their limiting values, C_{oo} and q_{oo} far upstream and C_{co} and q_{io} at $x' = 0$, due to the changes in the flow depth and velocity along this reach. It is of interest to calculate the ice concentration and discharge at the end of the jam to gain some idea of the variations q_i and C_c undergo along the approach reach. In moving coordinates the ice discharge is constant and is

$$q_i' = q_i + C_c t_i V_o; \quad q_i' = C_i t_i \left(\frac{q}{h} + V_o \right) \qquad (36)$$

which together with the alternate expression for q_i', Eq. 21, yields

$$C_c = C_{co} \frac{V_o + V_o}{V_o + \dfrac{q}{h}} \qquad (37)$$

and

$$q_i = q_{io} + C_{co} t_i V_o \left(1 - \frac{V_o + V_o}{V_o + \dfrac{q}{h}} \right) \qquad (38)$$

The values of C_c and q_i at the upstream end of the jam, C_{co} and q_{io}, respectively, are obtained by replacing h with H in Eqs. 37 and 38. The results of this calculation are shown in Fig. 8, where it is seen that $q_{io}/q_{oo} < 1$ due to the storage of liquid water and, therefore, also of ice in the approach reach. On the other hand, $C_{co}/C_{oo} > 1$, reflecting the backwater-reach storage of ice which accompanies the reduced ice discharge.

The limiting value for C_c if the floating ice remains one floe thick is unity, and it is doubtful that, for irregularly shaped floes C_c can increase above about 0.8–0.9. Larger values can occur only if the floes "shelve," i.e., override one another. Perhaps in reality C_c increases only to the neighborhood of unity before it produces bridging and resulting flow blockage and modification of the jam evolution to the extent that C_c does not become greater than a limiting value, somewhat less than unity.

Evolution to Equilibrium

The force balance relation for the ice and the mass and momentum-conservation equations derived previously in Eqs. 13, 17, and 18 are generally valid, but solutions were developed only for the equilibrium quasi-steady case. During the time the jam is evolving to equilibrium the governing equations cannot be solved so readily for several reasons. First, the partial differential equations cannot be reduced to ordinary differential equations by a simple transformation, because the jam profile does not move upstream with constant velocity. Second,

there is no generally valid downstream boundary conditions, as there is in the quasi-steady situation. Instead, the downstream condition is dictated by the nature of the local obstacle that initiates the jam. Similarly, it is not altogether clear what initial condition should be employed. In reality, most jams likely start as a single layer of arrested floes. But the previously developed formulation is not applicable until the accumulation acts as a continuum, i.e., until the embacle is several floes thick. In any event, it is doubtful that the effort required to obtain a general analytical description would be justified, since the evolutionary stage is of relatively short duration, and in view of the limited applicability of the formulation until the jam has thickened appreciably. It is fairly easy, however, to develop approximate estimates for the time required for a jam to achieve its equilibrium thickness, and for its length, downstream thickness, and rate of upstream propagation at any time during the evolutionary stage.

Time of Evolution to Equilibrium.—The time required for a jam to reach equilibrium thickness at its downstream end, T_{eq}, will be estimated under the assumption that the ice discharge (in fixed coordinates) at the upstream end of the jam varies linearly with time from its initial value, q_{ui}, to its final value, q_{uf}. The volume of ice in the jam when equilibrium is achieved, $\forall_{uf} h_u^2$, is equal to the ice discharged across the section reached by the leading edge of the jam up to the moment it reaches quasi-steady conditions, plus the volume of ice initially in the reach of length x_{uq}. Therefore

$$\forall_{uf} h_u^2 = \frac{q_{ui} + q_{uf}}{2} T_{eq} + x_{uq} C_{iu} t_i \quad \ldots\ldots\ldots\ldots\ldots\ldots\ldots\ldots\ldots\ldots\ldots\ldots\ldots\ldots\ldots\ldots\ldots\ldots (39)$$

Introducing the nondimensional time

$$T_{eq} = \frac{T_{eq}}{\frac{h_u^2}{q_u}} \quad \ldots\ldots\ldots\ldots\ldots\ldots\ldots\ldots\ldots\ldots\ldots\ldots\ldots\ldots\ldots\ldots\ldots\ldots (40)$$

into Eq. 39 and solving for T_{eq} yields

$$T_{eq} = \frac{2 q_u}{q_{ui} + q_{uf}} (\forall_{uf} - x_{uq} C_{iu} t_{ui}) \quad \ldots\ldots\ldots\ldots\ldots\ldots\ldots\ldots\ldots\ldots\ldots\ldots\ldots\ldots\ldots\ldots\ldots\ldots (41)$$

in which $t_{ui} = t_i / h_u$ = the normalized flow thickness; q_{ui} is obtained from Eq. 38 with h replaced by H; and x_{uq} and $\forall_{uf}$ can be obtained from Fig. 6. The quantities T_{eq} and T_{eq} are given in Fig. 9 as functions of C_{iu} for two different values of C_{iu} and k_s, and the flow, channel, and ice properties specified previously.

For calculation of estimated length, downstream thickness, and propagation velocity during evolution, a major assumption will be employed. The profile of an evolving embacle (one that has not reached equilibrium thickness at its downstream end) containing a volume of $\forall_u h_u^2$ of ice is the same as the profile of the quasi-steady jam, that eventually will form, between its upstream end, $x_u = 0$, and the station, $x_u(\forall_u)$, upstream from which it contains a volume, $\forall_u h_u^2$, of ice. This assumption is at best only approximately correct, for the streamwise distributions of shear stress on the bottom of the jam and of the weight of ice and pore water, and the momentum transferred to the upstream

end of the jam by the arriving floes, all of which determine jam profile, differ somewhat between evolving and the equilibrium embacles. Nevertheless, the assumption appears to be adequate for the purpose at hand, in view of the relatively short time occupied by the transient to the quasi-steady state (see Fig. 9). Further, it will be assumed, as in estimating the time of evolution to equilibrium, that the ice discharge (in fixed coordinates) at the upstream end of the embacle varies linearly with time.

Using these assumptions the time, $T(\forall_o)$, required for a volume $\forall_o h_a^2$ of ice to accumulate in the jam can be obtained from

$$\forall_o h_a^2 = \left[\frac{q_{im} + q_{io} \dfrac{T(\forall_o)}{T_{eq}}}{2} \right] T(\forall_o) + C_{ca} t_i x_o(\forall_o) h_a \qquad (42)$$

in which $\forall_o$ = the nondimensional volume of ice contained in the jam between $x_o = 0$ and $x_{oo} = x_o(\forall_o)$. Solving for T yields

$$T(\forall_o) = \frac{T_{eq}}{q_{io}} \left\{ -\frac{q_{im}^2}{2} + \left[\frac{q_{im}^2}{2} - 2 \frac{q_{io}}{T_{eq}} (C_{ca} t_i x_o h_a - \forall_o h_a^2) \right]^{1/2} \right\} \qquad (43)$$

The relation between $\forall_o$ and x_o, required for the application of Eq. 43, was obtained by integrating the thickness profile of the equilibrium embacle from its leading edge to $x_{oo}(\forall_{oo})$. This calculation is a part of the computer program developed by the first writer (11). Examples of this relation are given in Fig. 10 for two profiles, one of which appears in Fig. 4.

Estimates of jam length and downstream thickness as functions of time are obtained by: (1) Selecting values $\forall_o / \forall_{oo}$ and determining the corresponding values of x_o / x_{oo} from graphs of the type given in Fig. 10, but calculated for the jam under consideration; (2) determining $\forall_o$ and x_o from the known values of $\forall_{oo}$ and x_{oo}—the x_o so determined is the length of the jam at $T(\forall_o)$; (3) calculating $T(\forall_o)$ from Eq. 43 and (4) determining the thickness at the downstream end of the jam from the graphical relation between $\forall_o / \forall_{oo}$ and t_o / t_{oo}, an example of which is given in Fig. 10, calculated from the ice thickness profiles. This t_o, denoted by $t_o(T)$, is the estimate of the downstream thickness of the jam.

The velocity of propagation of an evolving jam, $V_s(T)$, can be estimated from the relation between x_o and $T(\forall_o)$ obtained from steps 2 and 3. It can also be estimated from the downstream thickness, the ice discharge, and surface concentration by means of the approximate ice-continuity relation

$$V_s(T) t_o(T) h_a (1 - p) = \left[\frac{q_{im} + q_{io} \dfrac{T(\forall_o)}{T_{eq}}}{2} \right] + V_s C_{ca} t_i \qquad (44)$$

the origin of which is immediately apparent if the jam is considered to be quasi-steady at any time and envisioned in coordinates moving upstream with velocity V_s. From Eq. 44 there results

$$V = \left[\frac{q_w - q_m \frac{T(\Psi_c)}{T_m}}{2} \right] \frac{1}{h_e t_e (T \times 1 - p) - C_m t_i} \quad (45)$$

in which $t_i(T)$ is determined in step 4 of the previously outlined procedure.

Summary and Conclusions

The analytical model of ice jams developed herein has treated jamming as a well-ordered phenomenon. It should be recalled that large natural jams are, at best, chaotic disorderly untidy affairs, as Fig. 1 and the photos presented by the first writer (11) attest. The results of the present or any other mathematical model of ice jams can be expected to predict only the global or general features of jams. However, this frequently is the type of information needed by river engineers confronted with actual or potential ice-jam problems.

The analysis is based, to the extent possible, on generally applicable principles of mechanics. The most tenuous step of the analysis is the adoption of linear relations between ice thickness and shear and compressive strengths, Eqs. 8 and 9, and the exclusion of the effects of strain rate on cover strength. The strain-rate dependence of jammed ice has some interesting implications for the formation of embacles. The deformation rate of an arrested ice accumulation must be greatest near the upstream end of the jam and diminish to zero at $x_c = x_m$ for quasi-steady jams. This suggests that k_x and C_o are not constant along the jam. However, the present state of understanding and the formulations of the strengths of fragmented ice are not yet sufficiently well developed to justify inclusion of the three strength coefficients as variables in the analytical model. Perhaps k_x, and C_o, and C_i, the only undetermined quantities in the analysis, should be regarded as coefficients that must be determined from relatively complete data on natural and laboratory jams. Data of this type would be most welcome for the verification of the present theory they would make possible, as well as for the quantification of the three strength coefficients they might provide.

Acknowledgment

The analytical and experimental results reported herein resulted from parts of more comprehensive investigations of river ice sponsored by the Rock Island District, U.S. Army Corps of Engineers, under Contract No. DAC25-73-C-0032, and by the National Science Foundation under Grant No. GK-3590X1.

Appendix I.—References

1. Ashton, G. D., "Entrainment of Ice Blocks—Secondary Influences," *Proceedings of the Symposium on River and Ice*, Paper A-11, International Association for Hydraulic Research, Budapest, Hungary, 1974.
2. Beckett, R., and Hurt, J., *Numerical Calculations and Algorithms*, McGraw-Hill Book Co., Inc., New York, N.Y., 1967, pp. 200-213.
3. Bojurnas, L., "Natural Regulation of the Great Lakes," *Proceedings of the Sixth Conference on Great Lakes Research*, Publication No. 10, Great Lakes Research Division, University of Michigan, Ann Arbor, Mich., 1963, pp. 183-189.

4 Carey, K. L., Ashton, G. D., and Frankenstein, G. E., "Ice Engineering for Civil Works," *Baseline Study*, United States Army Cold Regions Research and Engineering Laboratory, Hanover, N.H., 1973.
5 Frankenstein, G., "The Modification of a River to Prevent Ice Jams," United States Army, Cold Regions Research and Engineering Laboratory, Hanover, N.H., 1971.
6 Frankenstein, G., and Assur, A., "Israel River Ice Jam," *Proceedings of the Symposium on Ice and Its Action on Hydraulic Structures*, International Association for Hydraulics Research, 1972.
7 "Ice Conditions Winter 1965–1966," *After Action Report*, U.S. Army Corps of Engineers, Rock Island, Ill., 1967.
8 Lambe, T. W., and Whitman, R. V., *Soil Mechanics*, John Wiley and Sons, Inc., New York, N.Y., 1969.
9 Larsen, P., "Head Losses Caused by an Ice Cover on Open Channels," *Journal of Boston Society of Civil Engineers*, Vol. 56, No. 1, 1969, pp. 45–67.
10 Merino, M. P., "Internal Shear Strength of Floating, Fragmented Ice," thesis presented to the University of Iowa, at Iowa City, Iowa, in 1974, in partial fulfillment of the requirements for the degree of Master of Science.
11 Uzuner, M. S., "Hydraulics and Mechanics of River Ice-Jams," *Technical Report No. 161*, Institute of Hydraulic Research, University of Iowa, Iowa City, Iowa, 1974.
12 Uzuner, M. S., and Kennedy, J. F., "Stability of Floating Ice Blocks," *Journal of the Hydraulics Division*, ASCE, Vol. 93, No. HY12, Proc. Paper 9418, Dec., 1972, pp. 2117–2133.